POLITECNICO DI TORINO
Repository ISTITUZIONALE

Natural wastes as particle filler for poly(lactic acid)-based composites

(Article begins on next page)

25 April 2024

Natural wastes as particle filler for poly(lactic acid)-based composites

Daniele Battegazzore*, Amir Noori, Alberto Frache

Dipartimento di Scienza Applicata e Tecnologia, Politecnico di Torino, Alessandria site

Viale Teresa Michel 5, 15121 Alessandria, Italy

*Corresponding author: Tel/Fax: +390131229343/+390131229399; e-mail address: daniele.battegazzore@polito.it

Abstract

The paper describes the production and the mechanical characteristics of composites made completely of renewable raw materials. Several wastes or by-products from agro-industrial production namely hemp hurd , alfalfa and grape stem were analyzed in terms of thermal stability, morphological and chemical composition in an attempt to validate their use in composites. Such natural particle fillers were used in the range of 10 to 50 wt.-% in combination with poly(lactic acid) by melt blending to obtain fully bio-based composites. These fillers were responsible for a noteworthy increase in the storage modulus. Furthermore, two micromechanical models (namely, Voigt and Halpin-Tsai) were mathematically fitted the experimental data, and then the unknown moduli were extrapolated and compared with other fillers. Finally, the flexural strength of the bio-composites and an adhesion evaluation by exploiting Pukanszky's model were carried out. As a result, the hemp hurd in form of chips was the best investigated filler which showed the highest calculated modulus of 10.5 GPa (Voigt) and the best filler-matrix interaction with "B" -Pukanszky's coefficient - of 2.10. This information can be useful when comparison and selection of a suitable filler among the natural fillers are required.

Keywords:

Introduction

In the early days of composite development, fillers were added to polymers in order to lower the product price, enhance the composite mechanical properties and change the composite density. However, the increasing demands for plastic applications require the deployment of all possible filler advantages [1]. Natural fillers are renewable and cheaper alternatives to synthetic or inorganic ones and have several advantages such as low density and biodegradability [2, 3].

As far as the disposal of composites after the life cycle is concerned, using natural fillers with biopolymers can open a new horizon for a sustainable and eco-friendly industry. Moreover, the mechanical characteristics of the resulting bio-composites should be more or less at the same level as the conventional synthetic ones in order to replace them.

In this scenario, some bio-composites containing different natural fibers or particles have been comprehensively studied: cellulose fibers [4-11], abaca and jute fibers [5], flax fibers [10, 12-14], wood fibers [15, 16], hemp [17-20], kenaf [21, 22], cordenka fibers [14], bamboo fibers [23, 24], silk [25], wood flour [10, 16, 26], apple fibers [27, 28], pineapple [29, 30], cassava flours [29], banana [31], oat husks[27], cocoa shells[27, 32], sugar beets [28, 33], coconut shells [34], arundo donax [35], rice husk [20, 21, 36-38], corn cob [10], hazelnut shell [10], cotton by-products (cottonseed hulls and cotton burr) [39], hazelnut skins [32], chicken feather fiber [40], newspaper [41].

Natural fibers like cellulose, jute, hemp, sisal, flax, kenaf, silk have already been investigated extensively for bio-composite production with excellent results, but they generally cost a lot [42]. Therefore, the focus of this article is on the use of agricultural wastes, which are inexpensive, environment-friendly and abundantly available. Moreover, residues like straw, stalks, husk, trimming can be easily separated from other wastes, therefore, they are valued compared to the mixed solid wastes derived from residential and commercial activities. Nevertheless, a lot of agricultural residues have still not been investigated as a potential filler for polymers in order to maximize the positive effects and minimize the negative ones.

Hemp is a multi-purpose crop delivering fiber, hurd and seed. The fiber is used today for cigarette paper, insulation material and biocomposites. The hurd is the woody inner core of the stem which constitutes 60 wt.-% of the original plant, and it is mostly used for animal bedding and construction [43]. The use of this secondary product is at the center of this research.

Alfalfa is a widely grown plant throughout the world. It is mainly used as feed for cattle, horses, sheep, goats and other classes of domestic animals. It is a perennial herbaceous legume with a world production around 436 million tons in 2006 (FAO, 2006) [44]. In 2013 Italy was the third worldwide exporter in terms of quantity with more than 200 thousand tons (FAO, 2013) [44]. An overproduction of alfalfa leads to the collapse of the price and the consequent impossibility of handling and selling. It is not a waste or a by-product but it could realistically become an unsaleable material. Furthermore, it is

similar to other species of grasses thus it has been selected as an example of the use of grass or weeds directly into the polymers.

Grape belongs to the broadest fruit cultivation in the world, with about 69 million tons of global production from the FAO Statistical Database [44]. The biggest producers of table grapes are China, Turkey and Italy. Around 80% of the total crop is used in wine-making industry [45], consequently, in the countries like Italy, France, Spain with high wine production, a huge amount of waste is made. The grape stem is rich in bioactive polyphenols that are widely known for their antioxidant capacity [46]. The extraction of such substances has already been studied, but the use of these grape wastes in the polymers has not been considered. These types of natural fillers are examples of potential polymer fillers that have not yet been investigated so far.

The thermal stability of such organic wastes is limited and thus it is mandatory to select the polymer matrix with compatible processing temperatures. Among all the polymers, poly(lactic acid) (PLA) was chosen to make a completely bio-based and biodegradable composite and deep analyses on thermal degradation have been assessed.

The purpose of this article is to demonstrate the potential usefulness of bio-composites prepared with different agricultural wastes or by-products such as hemp hurd chips (HHC), hemp hurd powder (HHP), alfalfa (AA), and grape stem (GS). Different filler loadings were investigated in order to maximize the use of the wastes and minimize the use of the polymer. The thermo-mechanical properties were evaluated with DMTA.

A further goal of the work was to elaborate a mathematical model able to extrapolate the filler modulus from the composite experimental one. This can be extremely useful to predict the filler loading necessary to reach a performance desired for a selected application.

The strength of the bio-composites has also been investigated and used in the Pukanszky's model to evaluate the adhesion between fillers and matrix.

Material and methods

Materials

Poly(lactic acid) was provided by NatureWorks LLC (3051D grade).

Hemp Hurd in the form of Chips (hereafter abbreviated as HHC) and Powder (HHP) was provided by the local hemp association (AssoCanapa). Grape Stem (GS) was supplied by a winery in Piedmont province, then it milled twice to reach particle size lower than 5mm. Alfalfa (AA) was supplied by a local farm and ground as GS. All fillers details are reported in the Supplementary Information (Figure S1 and S2).

Both polymers and the fillers were dried at 80°C and 100°C respectively for 6 hours in a gravity convection oven before the melt blending.

Composite preparation

Composites with different filler contents (10,20,30,40 and 50 wt.-%) were melt blended by means of a co-rotating twin screw micro extruder DSM Xplore 15 ml Microcompounder. The micro extruder consists of a divisible fluid tight mixing compartment and two detachable, conical mixing screws. Residence time can be modified via recirculation of the melt and remained constant, for all the runs, at 5 min. In order to avoid the degradation of the polymer during the processing time, an N_2 purge flow was used. The screw speed was fixed at 50 rpm for feeding, and 100 rpm for the melt mixing and the heating temperature was set at 180°C. From here on, the samples have been abbreviated on the bases of the weight composition and the filler type: for instance, PLA20HHC stands for the composite containing 20 wt.-% of hemp hurd chips.

The specimens for dynamic-mechanical thermal analyses (DMTA) were produced by using a hot compression molding press at 180°C (PLA) of heating temperature and 10 MPa of pressure for 3 min obtaining 60x60x1 mm^3 plates. The final specimens for tests (6x30x1 mm^3) were derived from plates by razor blade cutting.

Characterization techniques

Thermogravimetric Analysis (TGA) was conducted using a Q500 TA Instruments analyzer. The samples (ca. 10 mg) were placed in open alumina pans, heated from 50 to 800°C at 10°C/min rate with a nitrogen flow of 60 ml/min. The collected data were $T_{10\%}$ (10% of weight loss), T_{max} (maximum weight loss rate), the residue at 600°C and the theoretical residue (CalR) calculated on the basis of the additivity rules for polymer blends (Equation 1).

$$CalR = R_f * x + R_p * (x - 1)$$

Equation 1

where R_f and R_p stand for the residue of neat filler and neat polymer at 600°C; x represents the filler weight percentage in the composites.

The Differential Scanning Calorimetry (DSC) analyses were carried out with a DSC Q20 supplied by TA Instruments. Samples of about 8 mg were heated at 10°C/min under nitrogen from 0°C to 200°C. The percentage crystallinity (X_c) of neat polymers and composites was calculated using Equation 2.

$$\chi_c(\%) = \frac{\Delta H_m - \Delta H_{cc}}{\Delta H_{100}(1 - x)} * 100$$

Equation 2

where ΔH_m and ΔH_{cc} are the melt and cold crystallization enthalpies obtained from the first heating scan, ΔH_{100} represents the melting enthalpy of the 100% crystalline polymer (93 J/g for PLA [47]) and x is the filler weight percentage.

Scanning Electron Microscope (SEM) micrographs were achieved with LEO 1400 VP Series (beam voltage: 20 kV; WD: 15mm) directly on the chopped wastes or on cross-sections of fractured composites in liquid nitrogen. The samples were metalized with gold. An X-ray probe (INCA Energy Oxford, Cu-Kα X-ray source, k=1.540562 Å) was utilized to do the elemental analysis.

Dynamic mechanical thermal analysis (DMTA) was conducted using a DMA Q800 TA Instruments. The following experimental conditions were chosen: temperature range from 30 to 120 ºC in air, heating rate of 3 ºC/min, 1 Hz frequency and 0.05% of oscillation amplitude in strain-controlled mode. The storage modulus (E') was measured with tension film clamp on 6x30x1 mm^3 samples.

In addition, a single cantilever test in isothermal condition (30°C) were performed with the same machine. A strain rate of 1%/min till the specimen rupture and a preload of 0.01% were set. Three samples were used for each formulation, the flexural modulus (E), maximum flexural strength (σ_{max}) and elongation-at-break (ε) averages and corresponding standard deviations were calculated.

Micromechanical modeling

Two models, namely Voigt (Equation 3) and Halpin-Tsai (Equation 4) have been taken into consideration in order to extrapolate the effect of the filler type and content in the prepared composites. For both models, the composite modulus (E_c) is determined from the filler (E_f) and matrix (E_m) moduli. Volumetric fractions (φ) are derived from the weight fractions calculated by using the density of each component attained from data sheets or derived by water and air weight measurements exploiting the Archimede's balance.

$$E_c = E_f \cdot \varphi_f + E_m \cdot \left(1 - \varphi_f\right)$$

Equation 3 Voigt model

$$\frac{E_c}{E_m} = \frac{1 + 2\eta\varphi_f}{1 - \eta\varphi_f} \quad \eta = \frac{\frac{E_f}{E_m} - 1}{\frac{E_f}{E_m} + 2}$$

Equation 4 Halpin-Tsai model

To predict and analyze yield stress, the most often applied correlation is credited to Nicolais and Narkis [48]. They presumed that the filler reduces the effective cross-section of the matrix which transfers the load during deformation. The model does not consider the effect of stress concentrations, assumes zero interaction and disregards all the other factors affecting yield stress. For this reason, another model from Pukanszky [49] that contemplates at least some of the neglected factors is used. This model employs a different expression for the effective load-bearing cross-section [50] and takes into consideration also the effect of interfacial interaction and interphase formation [51][49]. Specifically, Equation 6 derived from Equation 5, allows investigating a linear relation between the natural logarithm of reduced yield stress σ_{red} and the filler content [52][53].

$$\sigma_c = \sigma_m \cdot \frac{1 - \varphi_f}{1 + 2.5 \cdot \varphi_f} exp(B \cdot \varphi_f)$$

Equation 5 Pukanszky's model

$$\log(\sigma_{red}) = \log \frac{\sigma_c \cdot (1 + 2.5 \cdot \varphi_f)}{\sigma_m \cdot (1 - \varphi_f)} = B \cdot \varphi_f$$

Equation 6 Pukanszky's model

where σ_c and σ_m are the strength of the composite and matrix, respectively; B is a term corresponding to the load transferring competence of the filler and relies on filler-matrix interactions; and φ_f is the filler volumetric fraction within the polymer matrix.

Results and discussion

Wastes characterization

Thermal stability of wastes and natural products

Thermogravimetry analyses have been mainly conducted to check the thermal stability of the fillers at the PLA processing temperature. Figure 1a and b plot the filler weight loss and the weight loss rate as a function of temperature.

For all the fillers under investigation, the preliminary weight loss is because of the presence of water in the samples. For this reason, drying of these fillers before processing with the polymer matrix is essential; otherwise, it could facilitate polymer hydrolysis. Furthermore, the vertical dotted lines in Figure 1 illustrate that all fillers are stable at the chosen processing temperature (180°C). Using a polymer with a higher process temperature must be avoided because at 200°C a considerable weight loss is observed in Figure 1.

By analyzing the curves of weight loss rate in depth (Figure 1b), for all the fillers one peak is present from 314 to 350°C. Before this peak, a wide shoulder is clearly visible and can be ascribed to the presence of less thermally stable components. This shoulder, as well as the maximum peak value and shape, is useful information to hypothesize the composition of the wastes. Indeed, the main reported peaks are due to the cellulosic part of the natural wastes that generally shows only a sharp peak at 346°C in nitrogen for pure cotton, as reported in a previous work [10]. HCC and GS show this peak around this temperature (350 and 345°C, respectively), thus it is plausible to hypothesize the presence of cellulose. However, HHC has a really sharp peak while GS has a very broad and low peak. From this observation, HHC should have a higher percentage of cellulose than GS. On the other hand, AA and specially HHP present the main peak shifted to lower temperatures (327 and 314°C, respectively). These peaks could be ascribed to the cellulose but they were shifted because of the presence of other components that catalyze the cellulose degradation at lower temperatures. A second possible hypothesis is the presence of hemicellulose, which having shorter polymeric chain than cellulose, degrades at lower temperatures. This behavior has already been observed for corn cob [10]. Furthermore, other natural components could have lower

degradation temperatures with respect to cellulose. It has been reported that lignin starts degrading at above 200°C and loses mass quickly over a broad temperature range (up to around 400°C) and then keeps losing mass but at a slower rate [54]. Tannin degrades rapidly between 200°C and 300°C losing almost 20 wt.-% of its mass after which it continues to degrade but at a slower rate [54]. Similarly, starch has been reported to have a maximum degradation temperature around 310°C [10]. All of these components can be the cause of the shoulder presence before the main weight loss peak.

As far as residues were concerned, the cellulose gives a residue in nitrogen around 10% [10]. Starch, that has a chemical structure similar to cellulose, exhibits a similar residue (12%) [10]. Other types of wastes or by-products generate residues that are always higher than the neat cellulose (wood=27.5%, hazelnut=17.5%, corn cob= 23%, rice husk=36% hemp fibers=27% [10, 32, 36]). Newly, this fact is due to the other natural elements such as lignin, tannins, pectins, minerals and antioxidants present in the wastes that normally yield higher degradation residues. The final residue of HHC is the lowest (21%) that coupled with the highest peak of degradation, confirms cellulose as one of the main components. AA and HHP have a residue of 29% and 33%, respectively. They are ligno-cellulosic wastes similar to wood (W) or hemp fibers (H) with a lower amount of cellulose with respect to HHC. Finally, GS yields the highest residue (41%). This data in addition to the low intensity of the degradation peak, likely points out a low cellulose content.
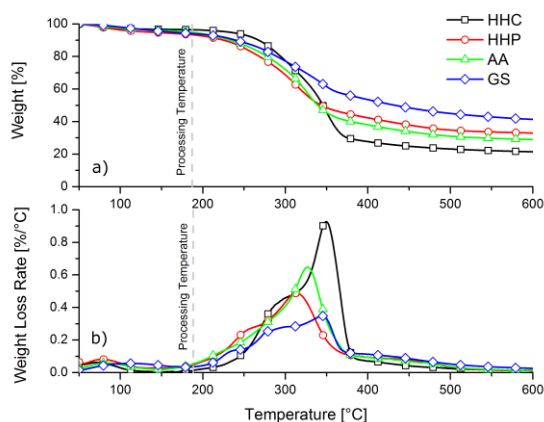

Figure 1. TG (a) and dTG (b) curves in nitrogen atmosphere of hemp hurd chips (HHC), hemp hurd powder (HHP), alfalfa(AA) and grape stem (GS).

Morphological and chemical characterization

The morphology and elemental analysis of the fillers are reported in Figure 2. The chopped natural wastes show a broad range of dimensions deeply reported in the Supplementary Information (Figure S1 and S2).

HHC has parallelepiped shape with length between 300 and 5000 μm and aspect ratio from 1 to 8. Some hemp short fibers are also present with aspect ratio till 18.

The HHP is a powder characterized by the presence of smaller particles than HHC. The bigger particles have a similar shape but dimensions from 100 to 700 µm and aspect ratios between 1 and 7, conversely, the smaller ones are globular (aspect ratio around 1) with diameters ranging between 30-100 µm. GS is morphologically similar to a mix of big fibers and particles. For this filler, it is hard to correctly define the length and aspect ratio because there are long branched fibers as well as big particles that are partially covered and tangled. Fibers of more than 5 mm length are also present as well as particles smaller than 300 µm.
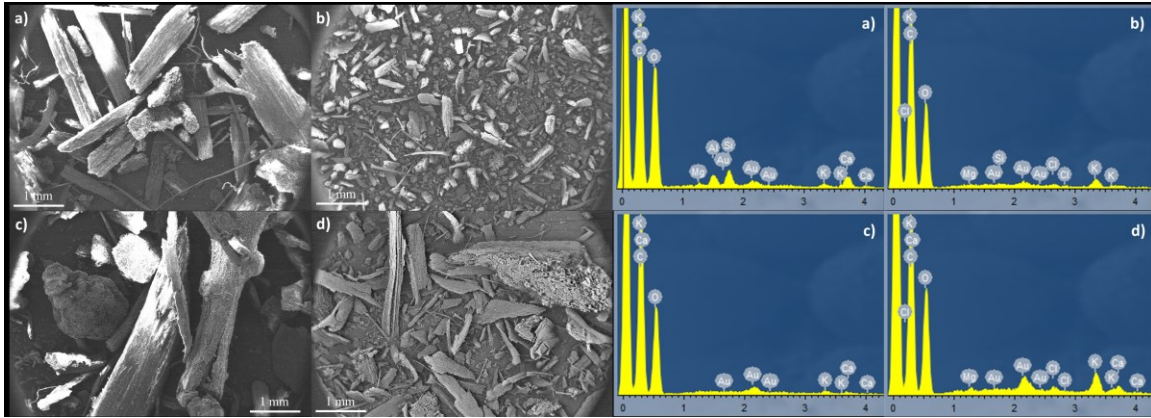

Figure 2. SEM magnifications and elemental analysis of hemp hurd chips (HHC) (a), powder (HHP) (b), grape stem (GS) (c) and Alfalfa(AA) (d).

AA is a heterogeneous mixture of fibers with length up to 3 mm and spherical particles from 0.2 to 1 mm. Indeed the resulting aspect ratios range broadly between 1 and 14.

In addition to the morphological analyses, the elemental analyses are reported in Figure 2. They show the obvious presence of C, H and O for the cellulose, hemicellulose and lignin, but also other elements are revealed: Mg, Al, Si, K, Ca, Cl as commonly found in natural products [55]. Comparing HHC and HHP, it is clear that the two fractions have similar chemical composition. A greater amount of Al, Si and Ca is found for the HHC while a higher amount of K in HHP. This difference can represent a further explanation of the different thermal degradation described in the TGA. GS, in addition to the expected C, H and O, has mainly K and Ca elements from carbonates. The same components are found in AA with the addition of Mg and Cl. Mg is related to the presence of chlorophyll that results in the intense green color of AA.

The elemental analyses demonstrated a great variability of metal elements which draws attention on the heterogeneity of the adopted fillers. This fact is an intrinsic characteristic of natural materials.

PLA-based composites

From the analyses carried out on the wastes or by-products, there are no reasons that they cannot be used in combination with polymer for industrial applications under 200°C, thus they were melt blended with PLA and compression molded in form of plates (Supplementary Information Figure S3).

Morphological analyses

The morphology of the produced composites has been probed with Scanning Electron Microscopy performed on the cross section of samples. Figure 3 reports SEM micrographs of PLA loaded with 10 wt.-% of hemp hurd chips (a), hemp hurd powder (b), alfalfa (c) and grape stem (d) at low and high magnifications. 10% loading has been selected as the representative condition in order to highlight differences in the adhesion and dimensions of the fillers.
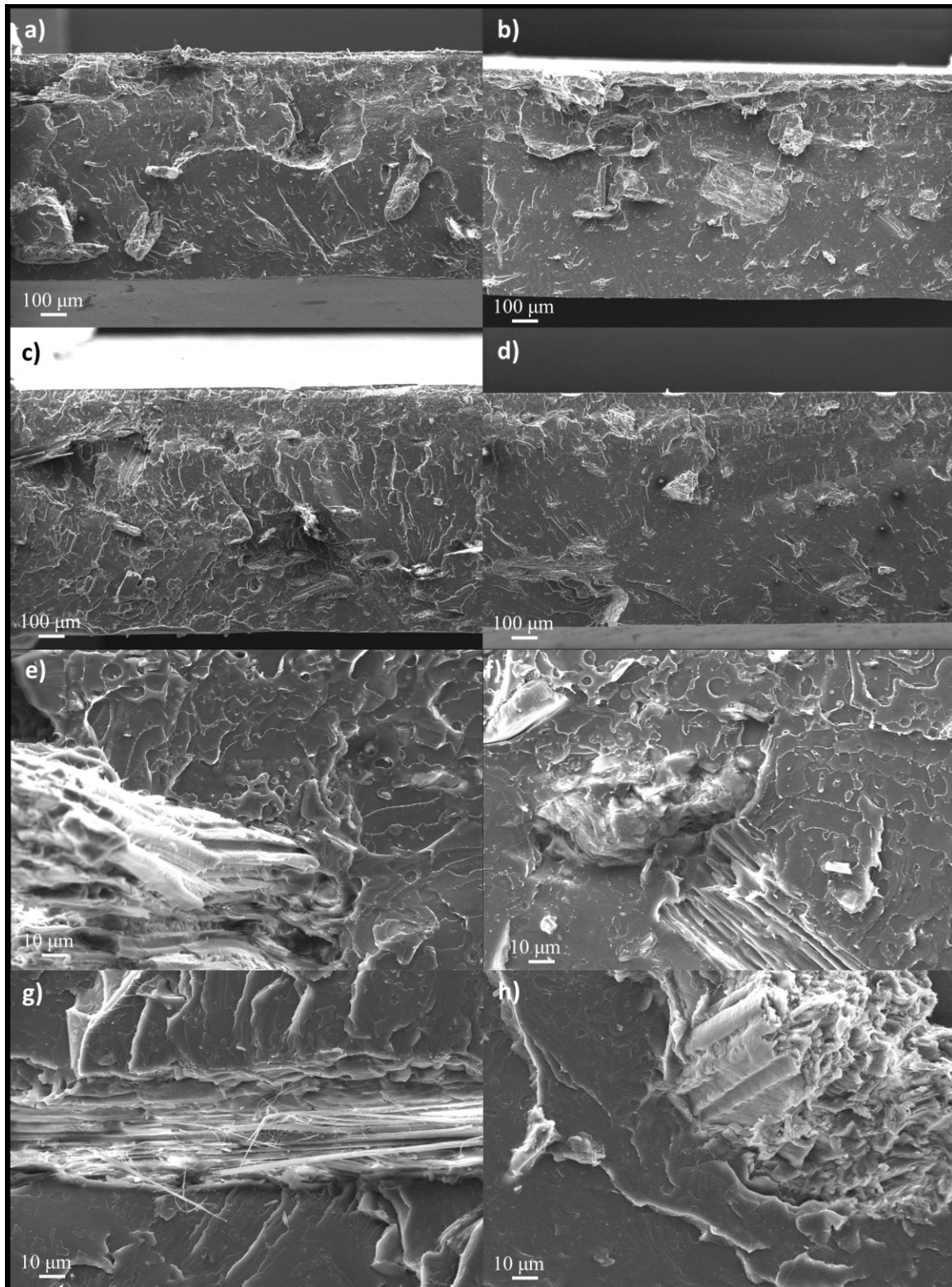
Figure 3. SEM micrograph at low (a-d) and high (e-h) magnifications of PLA loaded with 10 wt.-% of HHC (a,e), HHP (b,f), AA (c,g) and GS (d,h).

After the melt mixing, all the fillers under investigation show an inhomogeneous distribution of sizes as there was before compounding process. Despite this, a good adhesion to the polymer matrix seems to be achieved. From Figure 3, the distribution and dispersion of the fillers can be statistically determined by the position and the size of particles. In terms of distribution of the fillers into the matrix, almost all the fillers show a good result. No filler segregations are present but some empty areas are clearly visible because of the relatively low percentage of loading (10 wt.-%).

The broad distribution of sizes is maintained in the composites but the big particles are not more detected. Hence, particles breaking and dispersion during compounding have occurred but in case of HHC, AA and GS dimensions have remained between 50 and 400 μm. On the contrary, HHP shows little effect of the compounding process on the average particle size; this leads to a more homogenous distribution (30 - 200 μm).

The good interactions of HHC and GS (Figure 3e and h) with PLA are demonstrated by the adhesion of the polymer on the surface of the particles and lack of voids between filler and matrix. In the case of HHP and AA (Figure 3f and g), the adhesion between filler and matrix seems to be slightly better than HHC and GS as the particles were subjected to fracture on the same plane of the matrix. This points out that the stress transfers from the matrix to the filler with no pull-out or debonding effect.

It is important to underline that a great surface adhesion between filler and matrix was obtained without using any coupling agent. Indeed, Tran et al. [56] have already shown that the PLA matrix has a good interfacial adhesion with coir and flax fibers. This fact could be ascribed to the secondary bonds that are formed between the polar parts of the polymer chains and the natural wastes. On the other hand, also the shrinkage of the matrix could have an additive effect. Indeed, due to the mismatch in the thermal expansion coefficient between fillers and matrix, fillers are usually in compression state. This fact creates an adhesion between the two components even in the absence of any chemical bonds.

Thermal properties

TG data (reported in **Table 1**) demonstrate that all the fillers are responsible for $T_{10\%}$ and T_{max} anticipation with respect to the pure matrix. It is possible to observe a common trend for HHC, HHP and AA in which the $T_{10\%}$ and the T_{max} progressively decrease in proportion to the increase of filler content. The composites with GS point out a more undefined behavior probably due to the heterogeneity of the samples.

Notwithstanding the T_{max} of wastes and PLA are not very far, the wastes have less stable components that cause the anticipation of the composites degradation. Furthermore, it has been reported that metal components as present in the wastes can act as catalysts for the PLA degradation [57].

As far as the residues are concerned, by comparing the residue at 600 °C with the calculated one (CalR, obtained with the additive rule for polymer blends) in **Table 1**, it is

interesting to mention that HHC and HHP composites produce more char than expected which means fewer degradation products. Whereas, AA and GS composites demonstrate equal or lower residue than expected. This fact is not an interesting aspect for investigation in this article but it could be important if flame retardancy is concerned.

Table 1. TGA and DSC data of PLA-based bio-composites in nitrogen.

A second thermal property was also investigated: DSC (data reported in Table 1). Specifically, the evaluation of the materials crystallinity has been performed exploiting the first heating run of DSC analyses. The neat PLA is almost totally in the amorphous state (χ_c=3%). The percentage of crystallinity increases with the increase of the filler amount. In particular, a slight increase is registered with 10 or 30 wt.-% (1-10%) while a great enhancement is observed in the samples with 50 wt.-%, reaching χ_c=27%, 27%, 21% and 42% for HHC, HHP, AA and GS, respectively.

The occurrence of a nucleating effect of natural fibers on the crystallization of PLA is in agreement with the literature: PLA/hemp fiber composites [18], PLA/kenaf fiber composites [58], PLA/phormium tenax composites [59], PLA/pine wood flour composites [60] and PLA/coir fibers [61]. This effect could be significant for the mechanical and thermo-mechanical properties especially at high filler loadings.

Thermo-mechanical properties (DMTA)

DMTA in strain-controlled mode has been used in order to determine the effect of the filler type and content on the storage modulus (E') of the matrix. Figure 4 reports the trend of the storage modulus *vs*. temperature for 30 and 50 wt.-% filler content. All the other curves are reported in the Supplementary Information Figure S4.
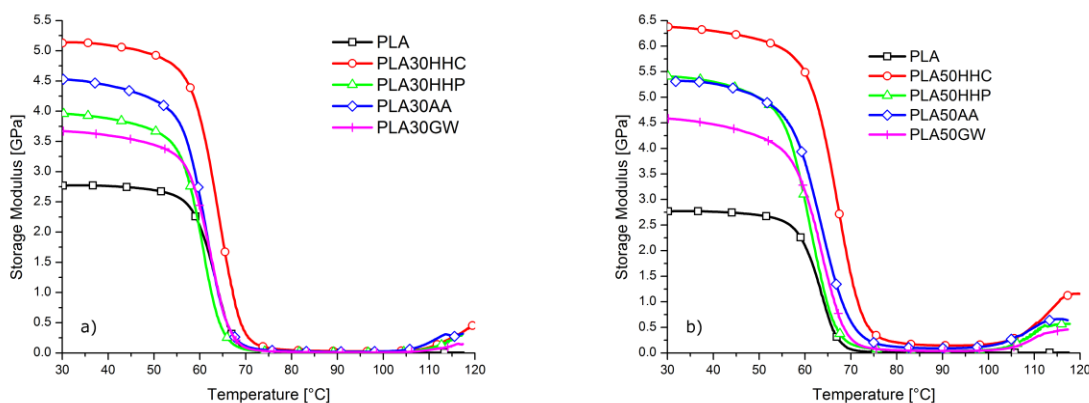

Figure 4. DMTA curves of PLA and corresponding bio-composites at 30 (a) and 50 (b) wt.-% of filler content

Firstly, regardless of the filler type, a significant increase of E' has been observed in the glassy region for all the composites. Every formulation has the glass transition region between 55°C and 75°C. HHC filler has demonstrated to be the most efficient

filler for improving PLA thermo-mechanical behavior, despite the fact that this increase is limited. It can be easily seen that the viscoelastic transition region of PLA50HHC is shifted by 10°C with respect to the pure PLA. This is a significant improvement for PLA-based composites due to the low T_g of PLA (60-65°C). At 67°C, the storage modulus of pure PLA drops to 0.25 GPa while PLA50HHC shows a storage modulus of 2.77 GPa that is comparable with the value registered for neat PLA at 30°C.

In order to have a deeper understanding on the behavior of such materials, the data of storage modulus at 30°C for all the formulations are listed in Table 2 (reported as a function of weight fraction).

Table 2. Storage modulus data of bio-composites at 30°C as a function of the filler content and type.

For instance, PLA30GS has the worse modulus increase with respect to neat PLA, but it is comparable to the same amount of corn cob found in a previous work [10]. However, at low filler content (10 wt.-%), GS raised the storage modulus by 22%, three times higher than cob (7%).

By drawing a comparison between HHP and cellulose short fibers reported in the literature [10], at 10 wt.-% filler content, the storage modulus increase of HHP composite is significantly higher than cellulose (30% vs 18%). When the amount of filler comes to 30 wt.-%, the trend is reversed but comparable (43% vs 48%).

AA has an increase similar to that recorded with HHP but with a surprisingly high value (+64%) at 30wt.%. The best performance increase is reached with the use of HHC for all the studied loadings even better than the direct use of the cellulose short fibers.

By comparing the performances of HHC- and HHP-based composites, PLA20HHC shows slightly higher storage modulus than PLA40HHP which contains twice the amount of filler. The filler with the supposed higher amount of cellulose is capable of better increasing the modulus of PLA. However, the presence of cellulose is not the only aspect that determines the result.

As discussed, the fillers used in this study show better performance when employed at low loadings with respect to the others used as references. Especially the HHC and HHP have a surprising 30% modulus increase at 10 wt.-%. Unfortunately, the same performances were not achieved at higher loadings, but they still remain comparable or superior to the wastes or by-products mentioned in the introduction and reported in Figure 5 [7, 10, 16, 21, 23, 24, 26, 27, 29, 33-37, 39-41].
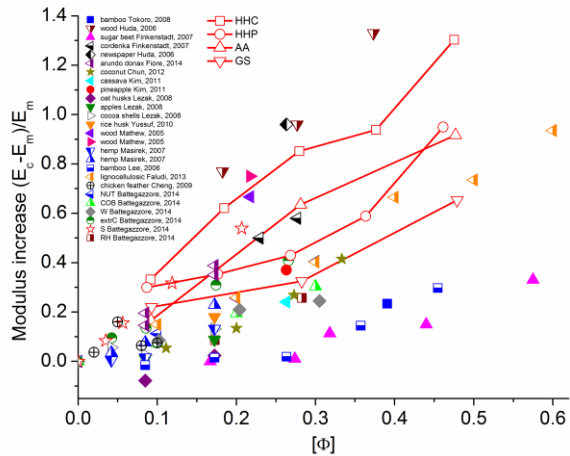
Figure 5. Comparison between the composites modulus increase with respect to the PLA matrix loaded with different wastes and by-products at different filler loading (Φ). The markers connected by lines are related to the composites studied in this research.

Storage modulus: structure-properties correlation

All the mechanical properties such as storage modulus are influenced by several aspects. In many cases, the modulus performance reduction occurs when the filler amount increases (Figure 5), and there are no deep explanations about this fact. This section is dedicated to the explication of the role of some parameters.

First of all, The variation in the crystallinity of the samples can be partially the cause of the mechanical properties changes even if there is not a linear correlation between the two effects. Generally, the increase in the crystallinity should give an increase in the modulus of the material. Pilla et al. [60] found an increase of crystallinity from 13 to 38% and 44% upon the addition of 20 and 40 wt.-% of filler for PLA/pine wood flour composites. They also report an increase in the modulus of the composites when a further increase in the crystallinity was reached with the addition of 0.5% of silane, but no changes in the mechanical properties were registered. In another study with PLA and waste leather buff, Ambone et al. [62] found no substantial differences in the crystallinity of the matrix and composites while he found changes in the moduli. Specifically, the tensile modulus increased from 2 wt.-% to 10 wt.-% of filler content while at higher content, the modulus was reduced.

One other hypothesis for the slight rise in tensile modulus could be explained based on filler dispersion. At low loading, the filler can be better dispersed and, consequently, stress transfer will be more efficient while at 30 wt.-% or above the filler starts to aggregate and acts as vulnerable points in the composites.

In order to explain this irregular trend, particles extracted from the HHC-based composites were analyzed by SEM. The length size distribution and the aspect ratio of the particles extracted from the formulations with 10, 30 and 50 wt.-% of fillers were evaluated. The statistical data are shown in Figure 6.
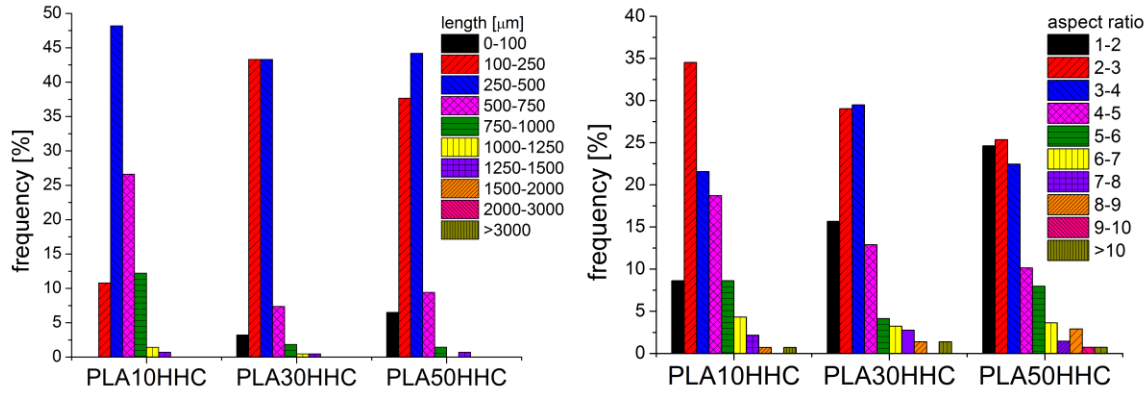
Figure 6. Length size and aspect ratio distribution [%] of the HHC particles extracted from the PLA-based formulations with 10, 30 and 50 wt.-% of fillers.

Due to the interactions between the filler particles and the processing shears, the distribution of filler size is averagely shifted to smaller statistical sampling moving from 10 to 50 wt.-%. However, negligible differences can be found between 30 and 50 wt.-%. Furthermore, the aspect ratio reveals more interesting insights as it shows a progressive increase in the fraction of particles having an aspect ratio between 1-2 at the expense of the others. The presence of particles with high aspect ratio (> 5) is maintained also at high filler loadings. From these data, it seems that the reduction of the average aspect ratio at high loadings can be considered as the main reason for the detrimental trend observed for HHC. On the other hand, at high filler loadings, the decrease of particle size and aspect ratio and the increase of agglomeration are partially mitigated by the increase in the crystallinity.

Voigt and Halpin-Tsai models application

The collected data at 30°C from DMTA have been discussed based on Voigt and Halpin-Tsai models in order to extrapolate the modulus of fillers. The usual exploiting of these two models is related to the evaluation of the composite modulus (E_c) when those of the matrix (E_m) and of the filler (E_f) are known. The evaluation of E_f was quite impossible since this is the first time that AA and GS have been investigated as natural fillers. Despite the fact that HHC and HHP have been already used, there are no studies to estimate the E_f. Therefore, the models previously explained have been applied reversely to calculate E_f on the basis of E_c data that collected experimentally from DMTA. To achieve this goal, the weight fractions (wt.-%) have been converted into volumetric fractions (φ), engaging the density values listed in Table 3. Neat PLA exhibits E_m value of 2.77 GPa. The E_f values calculated using the two models with the corresponding errors are listed in Table 3.

Table 3. Filler modulus (E_f) evaluated using Voigt and Halpin-Tsai models and error values (Error) from experimental data.

Figure 7 illustrates Voigt and Halpin-Tsai model calculations (full and dashed curves, respectively) as a function of the filler content, using E_f values listed in Table 3.

In the same figure, the DMTA experimental data are demonstrated with the uncertain bars.
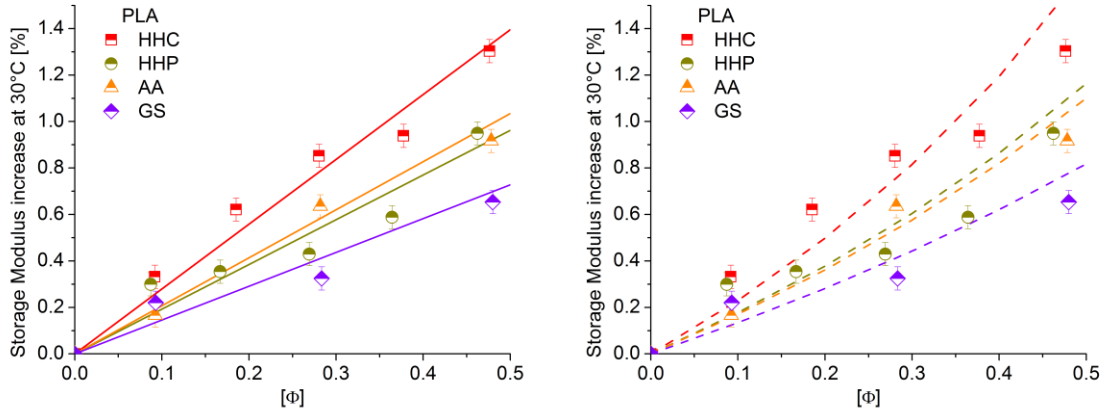

Figure 7. Storage modulus of PLA and corresponding bio-composites at 30°C as a function of the filler content (volumetric fraction ϕ), Voigt (full) and Halpin-Tsai (dotted) calculated curves.

The comparison between the calculated and experimental data (and taking into consideration the experimental error bars) highlights a not so close fitting of the two models. On the basis of Table 3 data, it can be concluded that Voigt model is able to give a more reliable evaluation of E_f with respect to Halpin-Tsai as the calculated error is always lower. However, even in the case where the Voigt model nearly approaches the experimental value, the calculated error is still 3.7% (AA in Table 3). Considering the curves in Figure 7, it seems that Voigt estimation (linear behavior) can better follow the data trend. On the other hand, Halpin-Tsai estimates an exponential rise of modulus increase which leads to an underestimation in stiffness at low filler loadings and an overestimation at high loadings.

The observed mismatch between the theoretical and experimental results may be due to the intrinsic limitation of use of these models as reported in the literature [60]. Indeed, these models do not account for the interface, for the variability in the modulus of the constituent materials and for the particles break.

Unfortunately, the corresponding calculated E_f for all the studied fillers are not available in the scientific literature, thus no comparison can be done. However, the obtained data through the Voigt model seem closer to the others which are reported in the literature for similar natural fillers (pineapple fiber 13.2 GPa [63], straws 8-9.3 GPa [64,65], cellulose 6.3 GPa, hazelnut 5.8 GPa, corn cob 5.0 GPa and wood 4.9 GPa [10]). It should be reminded that the Voigt model theorizes an optimum stress transfer between filler and matrix. As a consequence, the calculated value of E_f with this model is the lower boundary of the possible values which can be estimated by any other models.

Single cantilever mechanical tests and adhesion study

To give a more complete mechanical characterization to the materials, bending test with the single cantilever configuration was performed on DMTA instrument. Indeed, stiffness does not highly rely on interfacial adhesion, but very large differences are generally shown in tensile or flexural strength and elongation at break. The representative curves of the flexural tests for neat PLA and composites with 30 wt.-% or 50 wt.-% of filler were plotted in Figure 8 and statistical data results were listed in Table 4.
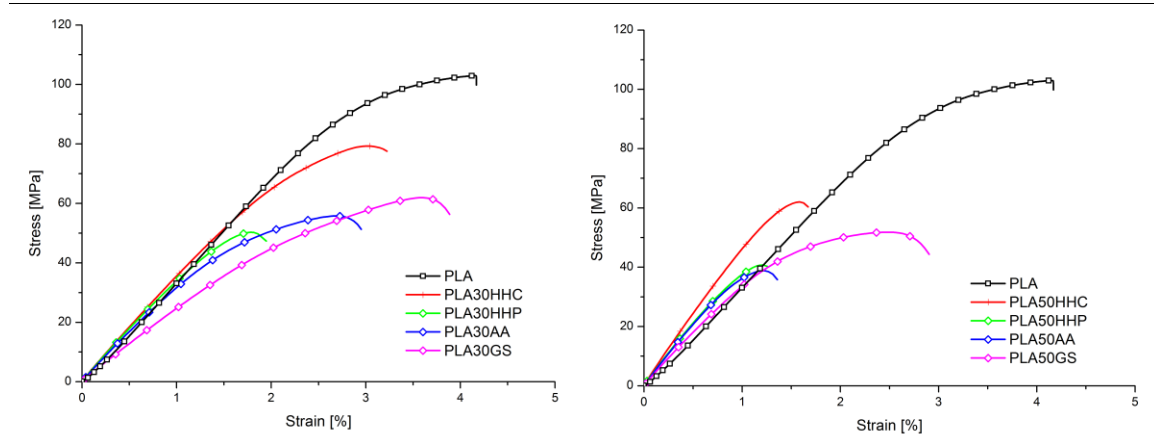

Figure 8. Stress-strain representative curves from single cantilever tests at DMTA on 30 wt.-% or 50 wt.-% of filler content.

PLA exhibits an average maximum stress of 101 MPa at deformation of 3.9%. At the end of the test, the specimen bent near the clamps without breakage into two separate parts. The addition of 30 wt.-% filler into the PLA matrix leads to a significant reduction in the maximum stress and the elongation at break. This behavior is even more apparent at the composites with 50 wt.-% filler content. By comparing all the composites, the best flexural strength for both loadings (30 and 50 wt.-%) was achieved with HHC filler (-23% and -35%, respectively) while GS achieved the highest deformation at break (+5% and -25%, respectively). The scatter plot reported in Figure 9 shows the flexural modulus as a function of the strength and can be useful for the correct selection of the material according to the applicative requests.
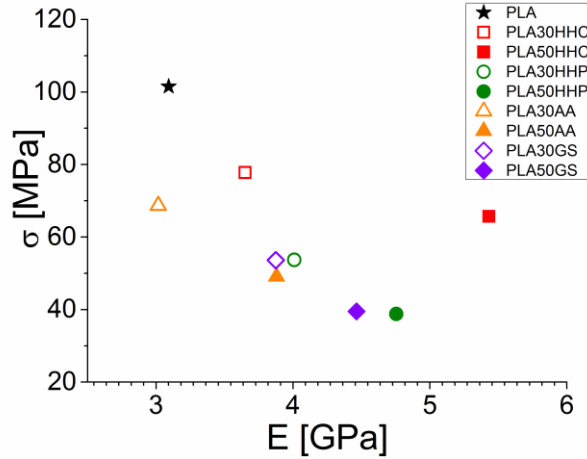
Figure 9. Flexural modulus (E) versus strength (σ) of PLA and composites.

Table 4. Single cantilever flexural test data.

The decrease in the stress at break in presence of a filler is a typical fact associated with a not perfect adhesion degree. On the other hand, the SEM analyzes and the increases in the composite moduli revealed a certain interaction between the matrix and the fillers. For this reason, it was decided to deepen this aspect with a study that is able to give a quantitative assessment of this stress transfer.

In Figure 10 the natural logarithm of reduced flexural stress (σ_{red}) as a function of the filler content (φ) is reported as well as the calculated B factor.

Again, the highest interaction is achieved with HHC (B= 2.10), the second position among the studied fillers is held by GS with a B value of 1.53. HHP and AA have the lowest behavior with B factor of 0.98 and 0.86, respectively. All the obtained values are greater than zero, a limit case that implies the lack of stress transfer.

Commercial silica particles in PLA (reported as "SIDI" and "S com" in Figure 10) have yielded B factors within 1.47 and 1.93 depending on their origin [36, 66]. Purified silica (S in Figure 10) extracted from rice husk has shown higher B factor (2.57) while the direct introduction of rice husk (RH in Figure 10) has given a similar result to GS (B=1.69) as reported in a recent paper [36]. Thus, the by-products or wastes used in this research revealed a capacity to carry the load similar to other agro-industrial by-products like rice husk even without any chemical or physical treatment for their modification.
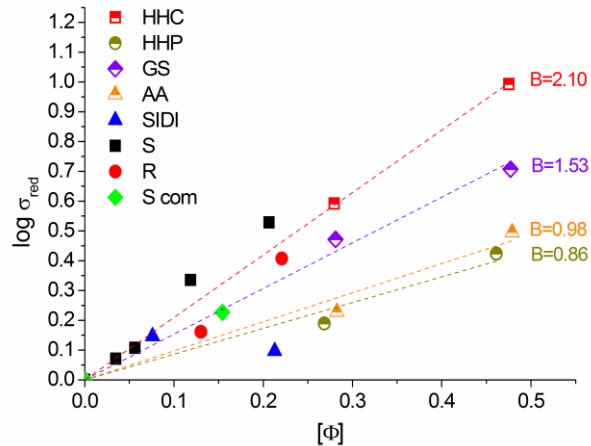
Figure 10. Reduced stress (σ_{red}) as a function of the filler volume fraction (Φ) of PLA-based composites and calculated B factor.

Conclusions

In the present work, four wastes or by-products which have not been sufficiently studied in the literature were considered for the direct use as filler in bio-matrices. Regardless of the filler type, there was no problem in terms of thermal stability at the PLA processing temperature. The TGA has proved to be a powerful tool for selecting and investigating the appropriate wastes to make bio-composites.

Hemp hurd chips (HHC), hemp hurd powder (HHP), alfalfa (AA), and grape stem (GS) were successfully melt compounded with poly(lactic acid) (PLA) from 10 to 50 wt.-% filler content.

DMTA in tension mode on composites has shown a strong increase of E' in the glassy region of PLA for all the formulations. The highest increase was obtained with 50 wt.-% of filler and the best overall performance was recorded by HHC-based composite (+130%). Voigt and Halpin-Tsai models were used to extrapolate the modulus of all fillers inside the composites under study. Voigt appeared to be the most suitable model to follow experimental data although errors were registered between 4 and 10%. These deviations from the models predictions are due to intrinsic limitations of the models themselves. Indeed, the mixing process and varying the filler quantity cause some changes in the matrix or fillers properties which are not considered in these models. Variation in the matrix crystallinity, filler particle size and aspect ratio, agglomeration and particles interactions are some of the causes which were presented and explained. It is not possible to separate the various contributions, but all of them have an effect on the final composite behavior. Nevertheless, the models predictions can be considered extremely useful information to evaluate/customize the filler content on the basis of a final application requirement. For instance, thanks to these elaborations, it is clear that only half the amount of HHC is needed to obtain the same result of HHP in terms of modulus.

Bending tests were also performed to give a more complete mechanical characterization to the materials. These tests gave the opportunity to analyze the interactions between the matrices and the fillers which were not considered in the mentioned models.

As expected from the addition of fillers, they increased the rigidity but decreased the strength and elongation at break (+76%, -35% and -55%, respectively for PLA50HCC). By applying the Pukanszky's equation to the composites strength, the highest filler-matrix interaction was achieved by HHC (B value of 2.10); thus, the best modulus increase is also reflected in the best interaction between the filler and the matrix. Furthermore, this by-product is also the one with the highest thermal stability and the one that is supposed to have the highest percentage of cellulose. Therefore, it seems that all these aspects correlate with the best final properties in the composite.

The mechanical data have shown that the investigated formulations can be technically used as materials for applications in various industries such as furnishings, decoration and packaging: to make boxes or containers. Furthermore, the appearance of these composites could be interesting for who is passionate about nature and natural fashion. This is while the environmental and economic advantages of valorizing such wastes could be appealing for others.

Finally, it was shown that not all the wastes act the same because the mechanical properties are influenced by many variables which are almost unforeseeable. This unpredictable behavior is the main reason why the use of each natural waste as filler requires extensive studies -like the one presented here- for a possible industrial exploitation.

Table 5. TGA and DSC data of PLA-based bio-composites in nitrogen.

Sample	$T_{onset10\%}$ [°C]	T_{max} [°C]	Residue at 600°C [%]	CalR [%]	χ_c [%]
PLA	331	350	1.9	-	3
HHC	268	350	21.4	-	-
PLA10HHC	305	327	5.3	3.8	6
PLA30HHC	295	325	9.5	7.7	4
PLA50HHC	272	296	14.2	11.6	27
HHP	225	314	32.9	-	-
PLA10HHP	267	290	6.0	5.0	1
PLA30HHP	247	268	11.7	11.2	7
PLA50HHP	241	264	19.5	17.4	27
AA	234	327	29.0	-	-
PLA10AA	260	285	5.1	4.6	4
PLA30AA	251	274	10.1	10.0	5
PLA50AA	247	268	15.6	15.4	21
GS	240	345	41.3	-	-
PLA10GS	254	267	7.1	5.8	7
PLA30GS	261	281	12.3	13.7	13
PLA50GS	254	276	17.6	21.6	42

Table 2. Storage modulus data of bio-composites at 30°C as a function of the filler content and type.

	Storage modulus at 30°C [GPa]					Δ [%][*]				
	10%	20%	30%	40%	50%	10%	20%	30%	40%	50%
HHC	3.69	4.49	5.13	5.37	6.38	33	62	85	94	130
HHP	3.60	3.75	3.96	4.40	5.40	30	35	43	59	95
AA	3.23	-	4.53	-	5.31	17	-	64	-	92
GS	3.38	-	3.67	-	4.58	22	-	32	-	65

* Δ = (E'composite-E'PLA)/E'PLA, where E'PLA = 2.77GPa

Table 3. Filler modulus (E_f) evaluated using Voigt and Halpin-Tsai models and error values (Error) from experimental data.

Filler	Density	Voigt model		Halpin-Tsai model	
	[g/cm^3]	E_f [GPa]	Error [%]	E_f [GPa]	Error [%]
HHC	1.38	10.5	6.4	23.3	10.0
HHP	1.46	8.1	10.1	13.3	11.2
AA	1.37	8.5	3.7	12.4	6.2
GS	1.36	6.8	7.0	9.0	7.8

Table 4. Single cantilever flexural test data.

Code	E [MPa]	ΔE [%]*	σ_{max} [MPa]	$\Delta\sigma_{max}$ [%]*	ε [%]	$\Delta\varepsilon$ [%]*
PLA	3092 ±123	-	101.5 ±3.0	-	3.9 ±0.5	-
PLA30HHC	3650 ±273	18.1	77.8 ±3.2	-23.3	3.3 ±0.2	-15.9
PLA50HHC	5431 ±85	75.6	65.7 ±3.7	-35.2	1.8 ±0.1	-54.6
PLA30HHP	4010 ±178	29.7	53.7 ±3.8	-47.0	2.1 ±0.2	-47.9
PLA50HHP	4754 ±205	53.8	38.8 ±4.0	-61.7	1.2 ±0.2	-70.6
PLA30AA	3874 ±313	25.3	53.6 ±3.0	-47.2	2.9 ±0.4	-26.8
PLA50AA	4464 ±564	44.4	39.5 ±2.6	-61.1	1.4 ±0.1	-64.7
PLA30GS	3016 ±430	-2.5	68.7 ±10.6	-32.3	4.2 ±0.5	5.1
PLA50GS	3880 ±373	25.5	49.1 ±2.8	-51.6	2.9 ±0.2	-25.2

*$\Delta X = (X\ composite-X\ PLA)/X\ PLA$

References

1. Móczó J and Pukánszky B. Particulate Fillers in Thermoplastics. In: Palsule S (ed) *Encyclopedia of Polymers and Composites*. Berlin, Heidelberg: Springer Berlin Heidelberg, 2014, pp.1-35.

2. Satyanarayana KG, Arizaga GGC and Wypych F. Biodegradable composites based on lignocellulosic fibers-An overview. *Progress in Polymer Science* 2009; 34: 982-1021. DOI: 10.1016/j.progpolymsci.2008.12.002.

3. Taj S, Munawar MA and Khan S. Natural fiber-reinforced polymer composites. *Proceedings-Pakistan Academy of Sciences* 2007; 44: 129.

4. Kowalczyk M, Piorkowska E, Kulpinski P, et al. Mechanical and thermal properties of PLA composites with cellulose nanofibers and standard size fibers. *Composites Part A: Applied Science and Manufacturing* 2011; 42: 1509-1514.

5. Bledzki A and Jaszkiewicz A. Mechanical performance of biocomposites based on PLA and PHBV reinforced with natural fibres–A comparative study to PP. *Composites science and technology* 2010; 70: 1687-1696.

6. Graupner N, Herrmann AS and Müssig J. Natural and man-made cellulose fibre-reinforced poly (lactic acid)(PLA) composites: An overview about mechanical characteristics and application areas. *Composites Part A: Applied Science and Manufacturing* 2009; 40: 810-821.

7. Mathew AP, Oksman K and Sain M. Mechanical properties of biodegradable composites from poly lactic acid (PLA) and microcrystalline cellulose (MCC). *Journal of Applied Polymer Science* 2005; 97: 2014-2025. DOI: 10.1002/app.21779.

8. Oksman K, Mathew AP, Bondeson D, et al. Manufacturing process of cellulose whiskers/polylactic acid nanocomposites. *Composites Science and Technology* 2006; 66: 2776-2784. DOI: 10.1016/j.compscitech.2006.03.002.

9. Braun B, Dorgan JR and Knauss DM. Reactively compatibilized cellulosic polylactide microcomposites. *Journal of Polymers and the Environment* 2006; 14: 49-58.

10. Battegazzore D, Alongi J and Frache A. Poly (lactic acid)-based composites containing natural fillers: thermal, mechanical and barrier properties. *Journal of Polymers and the Environment* 2014; 22: 88-98.

11. Huda M, Mohanty A, Drzal L, et al. "Green" composites from recycled cellulose and poly (lactic acid): Physico-mechanical and morphological properties evaluation. *Journal of Materials Science* 2005; 40: 4221-4229.

12. Zini E, Focarete ML, Noda I, et al. Bio-composite of bacterial poly (3-hydroxybutyrate-co-3-hydroxyhexanoate) reinforced with vegetable fibers. *Composites Science and Technology* 2007; 67: 2085-2094.

13. Oksman K, Skrifvars M and Selin JF. Natural fibres as reinforcement in polylactic acid (PLA) composites. *Composites Science and Technology* 2003; 63: 1317-1324. DOI: 10.1016/s0266-3538(03)00103-9.

14.   Bax B and Müssig J. Impact and tensile properties of PLA/Cordenka and PLA/flax composites. *Composites Science and Technology* 2008; 68: 1601-1607.

15.   Bogren KM, Gamstedt EK, Neagu RC, et al. Dynamic–mechanical properties of wood–fiber reinforced polylactide: experimental characterization and micromechanical modeling. *Journal of Thermoplastic Composite Materials* 2006; 19: 613-637.

16.   Faludi G, Hári J, Renner K, et al. Fiber association and network formation in PLA/lignocellulosic fiber composites. *Composites Science and Technology* 2013; 77: 67-73. DOI: 10.1016/j.compscitech.2013.01.006.

17.   Keller A. Compounding and mechanical properties of biodegradable hemp fibre composites. *Composites Science and Technology* 2003; 63: 1307-1316.

18.   Masirek R, Kulinski Z, Chionna D, et al. Composites of poly(L-lactide) with hemp fibers: Morphology and thermal and mechanical properties. *Journal of Applied Polymer Science* 2007; 105: 255-268. DOI: 10.1002/app.26090.

19.   Sawpan MA, Pickering KL and Fernyhough A. Improvement of mechanical performance of industrial hemp fibre reinforced polylactide biocomposites. *Compos Part a-Appl S* 2011; 42: 310-319. DOI: 10.1016/j.compositesa.2010.12.004.

20.   Battegazzore D, Alongi J, Duraccio D, et al. All Natural High-Density Fiber- and Particleboards from Hemp Fibers or Rice Husk Particles. *Journal of Polymers and the Environment* 2018; 26: 1652-1660. DOI: 10.1007/s10924-017-1071-9.

21.   Yussuf AA, Massoumi I and Hassan A. Comparison of Polylactic Acid/Kenaf and Polylactic Acid/Rise Husk Composites: The Influence of the Natural Fibers on the Mechanical, Thermal and Biodegradability Properties. *Journal of Polymers and the Environment* 2010; 18: 422-429. DOI: 10.1007/s10924-010-0185-0.

22.   Pan P, Zhu B, Kai W, et al. Crystallization behavior and mechanical properties of bio-based green composites based on poly (L-lactide) and kenaf fiber. *Journal of Applied Polymer Science* 2007; 105: 1511-1520.

23.   Lee S-H and Wang S. Biodegradable polymers/bamboo fiber biocomposite with bio-based coupling agent. *Composites Part A: Applied Science and Manufacturing* 2006; 37: 80-91. DOI: 10.1016/j.compositesa.2005.04.015.

24.   Tokoro R, Vu DM, Okubo K, et al. How to improve mechanical properties of polylactic acid with bamboo fibers. *Journal of Materials Science* 2008; 43: 775-787.

25.   Cheung H-Y, Lau K-T, Tao X-M, et al. A potential material for tissue engineering: Silkworm silk/PLA biocomposite. *Composites Part B: Engineering* 2008; 39: 1026-1033.

26.   Huda M, Drzal L, Misra M, et al. Wood-fiber-reinforced poly (lactic acid) composites: evaluation of the physicomechanical and morphological properties. *Journal of Applied Polymer Science* 2006; 102: 4856-4869.

27.   Lezak E, Kulinski Z, Masirek R, et al. Mechanical and thermal properties of green polylactide composites with natural fillers. *Macromolecular bioscience* 2008; 8: 1190-1200. DOI: 10.1002/mabi.200800040.

28.	Mohamed AA, Finkenstadt V and Palmquist D. Thermal properties of extruded/injection-molded poly (lactic acid) and biobased composites. *Journal of applied polymer science* 2008; 107: 898-908.

29.	Kim K-W, Lee B-H, Kim H-J, et al. Thermal and mechanical properties of cassava and pineapple flours-filled PLA bio-composites. *Journal of thermal analysis and calorimetry* 2011; 108: 1131-1139.

30.	Kaewpirom S and Worrarat C. Preparation and properties of pineapple leaf fiber reinforced poly(lactic acid) green composites. Fibers and Polymers 2014; 15: 1469-1477. journal article. DOI: 10.1007/s12221-014-1469-0.

31.	Shih Y-F and Huang C-C. Polylactic acid (PLA)/banana fiber (BF) biodegradable green composites. *Journal of Polymer Research* 2011; 18: 2335-2340. journal article. DOI: 10.1007/s10965-011-9646-y.

32.	Battegazzore D, Bocchini S, Alongi J, et al. Plasticizers, antioxidants and reinforcement fillers from hazelnut skin and cocoa by-products: Extraction and use in PLA and PP. *Polymer Degradation and Stability* 2014; 108: 297-306.

33.	Finkenstadt VL, Liu L and Willett J. Evaluation of poly (lactic acid) and sugar beet pulp green composites. *Journal of Polymers and the Environment* 2007; 15: 1-6.

34.	Chun KS, Husseinsyah S and Osman H. Mechanical and thermal properties of coconut shell powder filled polylactic acid biocomposites: effects of the filler content and silane coupling agent. *Journal of Polymer Research* 2012; 19: 9859. journal article. DOI: 10.1007/s10965-012-9859-8.

35.	Fiore V, Botta L, Scaffaro R, et al. PLA based biocomposites reinforced with Arundo donax fillers. *Composites Science and Technology* 2014; 105: 110-117. DOI: http://dx.doi.org/10.1016/j.compscitech.2014.10.005.

36.	Battegazzore D, Bocchini S, Alongi J, et al. Rice husk as bio-source of silica: preparation and characterization of PLA–silica bio-composites. *RSC Advances* 2014; 4: 54703-54712.

37.	Battegazzore D, Bocchini S, Alongi J, et al. Cellulose extracted from rice husk as filler for poly (lactic acid): preparation and characterization. *Cellulose* 2014; 21: 1813-1821.

38.	Battegazzore D, Alongi J, Frache A, et al. Layer by Layer-functionalized rice husk particles: A novel and sustainable solution for particleboard production. *Materials Today Communications* 2017; 13: 92-101. DOI: 10.1016/j.mtcomm.2017.09.006.

39.	Sutivisedsak N, Cheng H, Dowd M, et al. Evaluation of cotton byproducts as fillers for poly (lactic acid) and low density polyethylene. *Industrial crops and products* 2012; 36: 127-134.

40.	Cheng S, Lau K-t, Liu T, et al. Mechanical and thermal properties of chicken feather fiber/PLA green composites. *Composites Part B: Engineering* 2009; 40: 650-654. DOI: http://dx.doi.org/10.1016/j.compositesb.2009.04.011.

41.   Huda MS, Drzal LT, Mohanty AK, et al. Chopped glass and recycled newspaper as reinforcement fibers in injection molded poly (lactic acid)(PLA) composites: a comparative study. *Composites Science and Technology* 2006; 66: 1813-1824.

42.   Dittenber DB and GangaRao HVS. Critical review of recent publications on use of natural composites in infrastructure. *Composites Part A: Applied Science and Manufacturing* 2012; 43: 1419-1429. DOI: https://doi.org/10.1016/j.compositesa.2011.11.019.

43.   Carus M, Karst S, Kauffmann A, et al. The European Hemp Industry: Cultivation, processing and applications for fibres, shivs and seeds. *European Industrial Hemp Association (EIHA), Hürth (Germany)* 2013.

44.   STAT F. FAOSTAT-Statistical Database, 2012. 2012.

45.   Maier T, Schieber A, Kammerer DR, et al. Residues of grape (Vitis vinifera L.) seed oil production as a valuable source of phenolic antioxidants. *Food Chemistry* 2009; 112: 551-559.

46.   Anastasiadi M, Pratsinis H, Kletsas D, et al. Grape stem extracts: Polyphenolic content and assessment of their in vitro antioxidant properties. *LWT-Food Science and Technology* 2012; 48: 316-322.

47.   Garlotta D. A literature review of poly(lactic acid). *Journal of Polymers and the Environment* 2001; 9: 63-84. DOI: Unsp 1566-2543/01/0400-0063/0

Doi 10.1023/A:1020200822435.

48.   Nicolais L and Narkis M. Stress-strain behavior of styrene-acrylonitrile/glass bead composites in the glassy region. *Polymer Engineering & Science* 1971; 11: 194-199.

49.   Pukanszky B. Influence of interface interaction on the ultimate tensile properties of polymer composites. *Composites* 1990; 21: 255-262.

50.   Turcsanyi B, Pukanszky B and Tüdõs F. Composition dependence of tensile yield stress in filled polymers. *Journal of Materials Science Letters* 1988; 7: 160-162.

51.   Móczó J and Pukánszky B. Polymer micro and nanocomposites: structure, interactions, properties. *Journal of Industrial and Engineering Chemistry* 2008; 14: 535-563.

52.   Dorigato A, Sebastiani M, Pegoretti A, et al. Effect of Silica Nanoparticles on the Mechanical Performances of Poly(Lactic Acid). *Journal of Polymers and the Environment* 2012; 20: 713-725. DOI: 10.1007/s10924-012-0425-6.

53.   Lazzeri A and Phuong VT. Dependence of the Pukánszky's interaction parameter B on the interface shear strength (IFSS) of nanofiller- and short fiber-reinforced polymer composites. *Composites Science and Technology* 2014; 93: 106-113. DOI: 10.1016/j.compscitech.2014.01.002.

54.   Anwer MAS, Naguib HE, Celzard A, et al. Comparison of the thermal, dynamic mechanical and morphological properties of PLA-Lignin & PLA-Tannin particulate green composites. *Composites Part B: Engineering* 2015; 82: 92-99. DOI: 10.1016/j.compositesb.2015.08.028.

55.　　Fuqua MA, Huo SS and Ulven CA. Natural Fiber Reinforced Composites. *Polymer Reviews* 2012; 52: 259-320. DOI: 10.1080/15583724.2012.705409.

56.　　Tran L, Yuan X, Bhattacharyya D, et al. Fiber-matrix interfacial adhesion in natural fiber composites. *International Journal of Modern Physics B* 2015; 29: 1540018.

57.　　Aoyagi Y, Yamashita K and Doi Y. Thermal degradation of poly[(R)-3-hydroxybutyrate], poly[ε-caprolactone], and poly[(S)-lactide]. *Polymer Degradation and Stability* 2002; 76: 53-59. DOI: https://doi.org/10.1016/S0141-3910(01)00265-8.

58.　　Lee B-H, Kim H-S, Lee S, et al. Bio-composites of kenaf fibers in polylactide: Role of improved interfacial adhesion in the carding process. *Composites Science and Technology* 2009; 69: 2573-2579. DOI: 10.1016/j.compscitech.2009.07.015.

59.　　De Rosa I, Iannoni A, Kenny J, et al. Poly (lactic acid)/Phormium tenax composites: Morphology and thermo-mechanical behavior. *Polymer Composites* 2011; 32: 1362-1368.

60.　　Pilla S, Gong S, O'Neill E, et al. Polylactide-pine wood flour composites. *Polymer Engineering & Science* 2008; 48: 578-587.

61.　　Dong Y, Ghataura A, Takagi H, et al. Polylactic acid (PLA) biocomposites reinforced with coir fibres: Evaluation of mechanical performance and multifunctional properties. *Composites Part A: Applied Science and Manufacturing* 2014; 63: 76-84.

62.　　Ambone T, Joseph S, Deenadayalan E, et al. Polylactic Acid (PLA) Biocomposites Filled with Waste Leather Buff (WLB). *Journal of Polymers and the Environment* 2017; 25: 1099-1109.

63.　　Luo S and Netravali A. Mechanical and thermal properties of environment-friendly "green" composites made from pineapple leaf fibers and poly (hydroxybutyrate-co-valerate) resin. *Polymer composites* 1999; 20: 367-378.

64.　　Ahankari SS, Mohanty AK and Misra M. Mechanical behaviour of agro-residue reinforced poly (3-hydroxybutyrate-co-3-hydroxyvalerate),(PHBV) green composites: A comparison with traditional polypropylene composites. *Composites Science and Technology* 2011; 71: 653-657.

65.　　White N and Ansell MP. Straw-reinforced polyester composites. *Journal of Materials Science* 1983; 18: 1549-1556.

66.　　Battegazzore D, Salvetti O, Frache A, et al. Thermo-mechanical properties enhancement of bio-polyamides (PA10.10 and PA6.10) by using rice husk ash and nanoclay. *Compos Part a-Appl S* 2016; 81: 193-201. DOI: 10.1016/j.compositesa.2015.11.022.

Supporting Information

Natural wastes as particle filler for poly(lactic acid)-based composites

Daniele Battegazzore*, Amir Noori, Alberto Frache

Dipartimento di Scienza Applicata e Tecnologia, Politecnico di Torino, Alessandria site

Viale Teresa Michel 5, 15121 Alessandria, Italy

*Corresponding author: Tel/Fax: +390131229343/+390131229399; e-mail address:
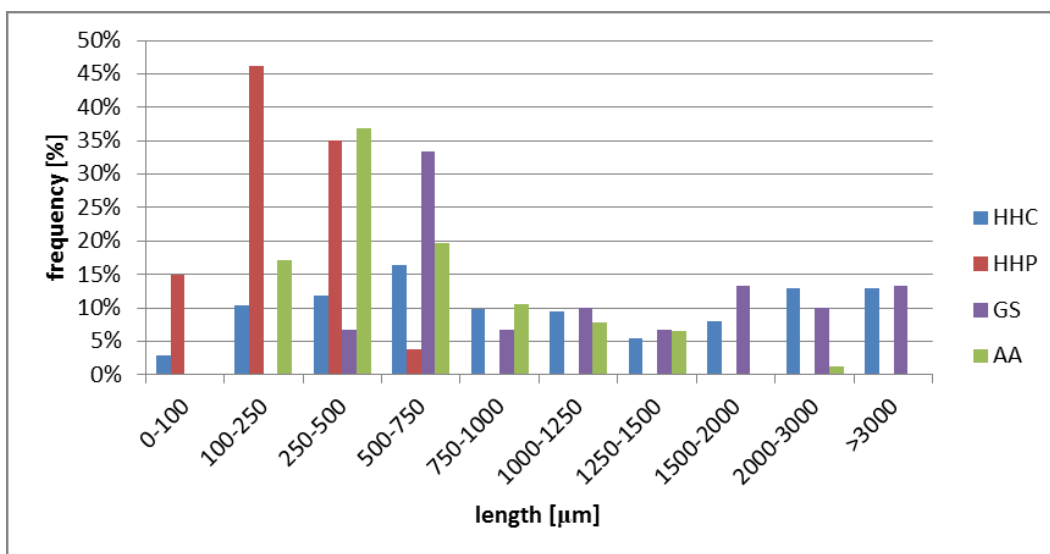
daniele.battegazzore@polito.it

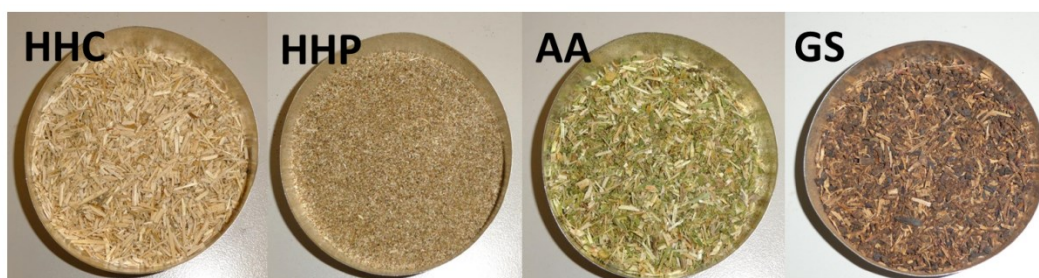**Figure S1 Distribution of dimensions of HHC, HHP, GS and AA before processing.**

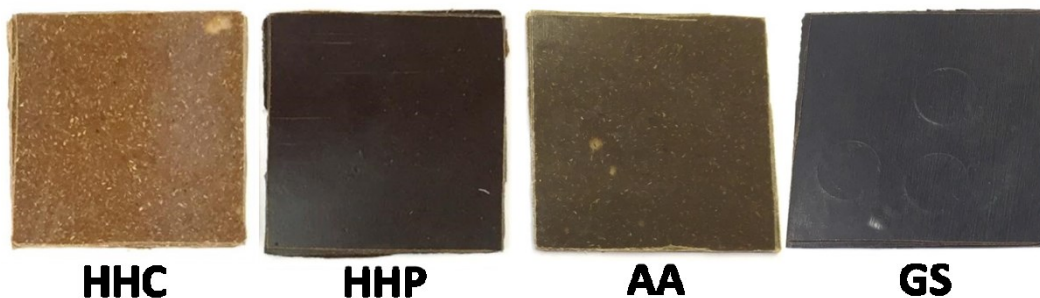**Figure S2 Visual appearance before extrusion of the wastes used (HHP, HHC, AA, GS).**

Figure S3 Compression molded plates of PLA-based composites with 30 wt.-% of fillers. Four major colors consist of light brown (HHC), dark brown (HHP), brown-green (AA), dark brown-purple (GS) and different particle shades with respect to different filler content can be designed.
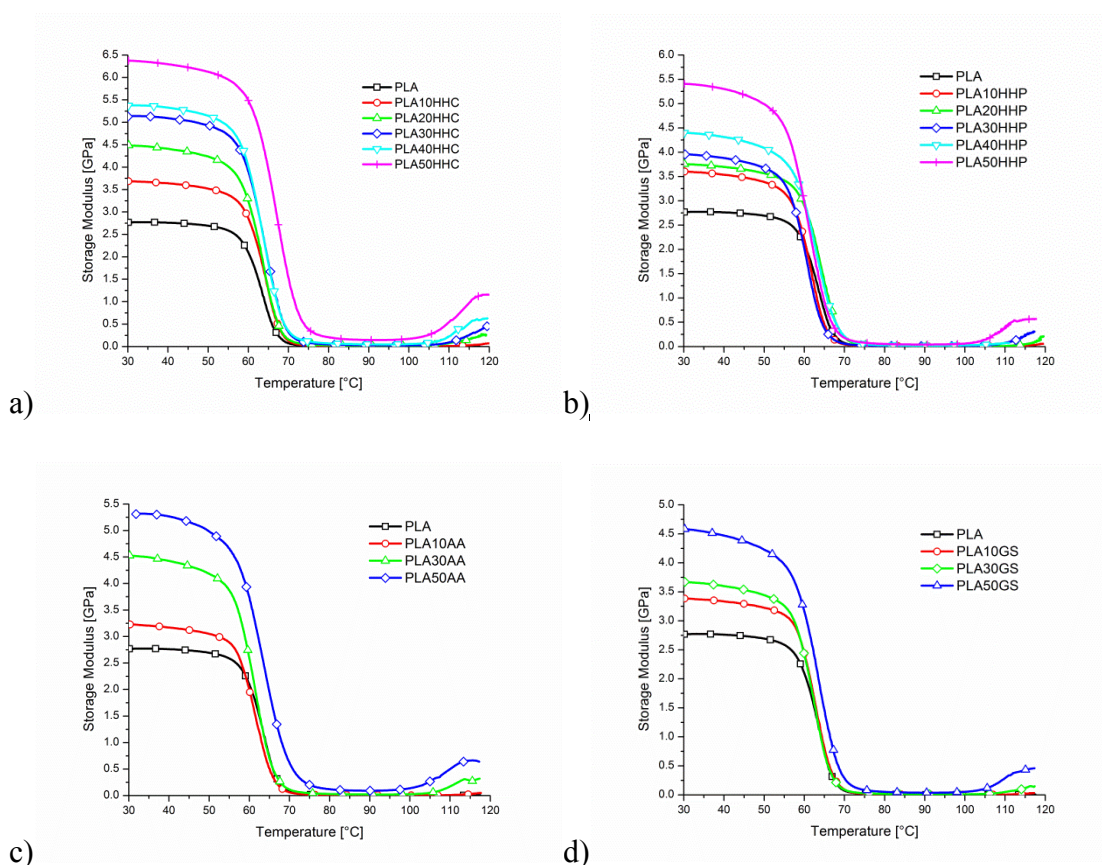

Figure S4. DMTA curves of PLA-HHC (a); HHP (b); AA (c) and GS (d) bio-composites at different fillers content